J. Serb. Chem. Soc. 70 (3) 513–525 (2005)
JSCS–3285

UDC 546.92+66.091.1:541.138:543.42
Original scientific paper

Platinum monolayer electrocatalysts for oxygen reduction: effect of substrates, and long-term stability

J. ZHANG,[1] M. B. VUKMIROVIĆ,[1] K. SASAKI,[1] F. URIBE[2] and R. R. ADŽIĆ[1*#]

[1]*Department of Materials Science, Brookhaven National Laboratory, Upton, NY 11973, USA (e-mail: adzic@bnl.gov) and* [2]*Los Alamos National Laboratory, Los Alamos, NM 87545, USA*

(Received 16 December 2004)

Abstract: We describe a novel concept for a Pt monolayer electrocatalyst and present the results of our electrochemical, X-ray absorption spectroscopy, and scanning tunneling microscopy studies. The electrocatalysts were prepared by a new method for depositing Pt monolayers involving the galvanic displacement by Pt of an underpotentially deposited Cu monolayer on substrates of Au (111), Ir(111), Pd(111), Rh(111) and Ru(0001) single crylstals, and Pd nanoparticles. The kinetics of O_2 reduction showed significant enhancement with Pt monolayers on Pd(111) and Pd nanoparticle surfaces in comparison with the reaction on Pt(111) and Pt nanoparticles, respectively. This increase in catalytic activity is attributed partly to the decreased formation of PtOH, as shown by *in situ* X-ray absorption spectroscopy. The results illustrate that placing a Pt monolayer on a suitable substrate of metal nanoparticles is an attractive way of designing better O_2 reduction electrocatalysts with very low Pt contents.

Keywords: electrocatalysis, oxygen reduction, platinum, monolayers, stability.

INTRODUCTION

As interest in a hydrogen-based economy grows, research is expanding on its major elements, *viz.,* hydrogen production, and storage and energy conversion in fuel cells.[1] Electrocatalytic oxygen reduciton, the reaction at fuel-cell cathodes, has been the focus of considerable attention because of its slow kinetics and the need for better electrocatalysts with decreased Pt content.[2–4] A particularly troubling feature of this reaction is the large loss in potential of 0.3–0.4 V during the initial part of the polarization curves that is the source of a major decline in the fuel cell's efficiency. Part of this polarization was attributed to the inhibition of O_2 reduction caused by OH adsorption on Pt in the potential region of 0.75 – 1 V.[3,5]

To alleviate these impediments, we developed a new approach to designing the low-Pt electrocatalysts for the cathode[6–10] and for the anode.[11,12] This approach involves depositing a Pt sub-monolayer or monolayer on suitable substrtes

* Author for correspondence.
\# Serbian Chemical Society active member.

of carbon-supported metal nanoparticles. We developed two methods of deposition. In the first,[6,7] the Pt submonolayer is deposited in an electroless (spontaneously) fashion on suitable substrate, while, in the other,[13] Pt is laid down by the redox replacement of a Cu monolayer. Both methods form Pt deposits in which all Pt atoms can be involved in the catalytic reaction. Consequently, Pt loading can be greatly reduced compared with other catalysts.

The catalytic properties of bimetallic surfaces consisting of metal monolayers on single-crystal metal surfaces have been extensively studied in ultra-high vacuum systems[14] and, to a lesser extent, in electrochemical ones.[15–18] In many cases, the formation of a surface metal–metal bond signficantly changed the electronic properties of the metal overlayer, and pronounced differences were observed in the reactivity of some transition metal monolayers on various substrates.[14] Norskov and coworkers recently proposed a description of the activity of metal monolayers,[19,20] according to which the characteristics of the surface metal d-bands, particularly the weighted center of the d-band (ε_d) play a decisive role in determining surface reactivity. Density functional theory (DFT) calculations showed that the binding energies and reactivity of small adsorption correlate well with the position of ε_d on strained surfaces and metal overlayers,[21] in accord with data from numerous experimental studies.[22–24] The framework of that description is implemented in the present study to elucidate trends governing the behavior of Pt monolayers deposited on the surfaces of other transition metals.

In the present communication we describe the kinetics of the O_2 reduction reaction (ORR) of a Pt monolayer on several single-crystal electrodes and on carbon-supported Pd nanoparticle electrocatalysts. A rotating disk or disk–ring electrode (RRDE) technique was used for the majority of the electrochemical measurements. The long-term test was carried out in a 50 cm^2 fuel cell. The data obtained using *in situ* X-ray absorption spectroscopy (XAS) measurement, *i.e.*, X-ray absorption near edge structure (XANES), rationalize the origins of the high catalytic activity for O_2 reduction. We emphasize that this XAS study provided unique spectra obtained only from the monolayer of Pt atoms on the surface of the metal nanoparticles, which take part in electrocatalytic reaction. These data facilitate a direct comparison between electronic/structural properties and catalytic activity. Previous data on Pt and Pt alloys were predominantly determined by the Pt atoms in the bulk material.

EXPERIMENTAL

The ORR electrocatalysts were prepared by our new method for depositing Pt monolayers involving the galvanic displacement by Pt of an underpotentially deposited (upd) Cu monolayer[13] on the surfaces of single crystal of Au(111), Rh(111), Pd(111), Ru(0001), and Ir(111), and on Pd nanoparticles deposited on glassy carbon disk. The Rh(111), Pd(111), Ru(0001) and Ir(111) crystals were mechanically polished with diamond pastes and alumina down to 0.05 μm and annealed by inductive heating in an Ar atmosphere. The surface preparation for Au (111) followed a standard procedure involving electropolishing and flame annealing. Immediately after depositing a Cu upd monolayer from deoxygenated 0.05 M $CuSO_4$ in a 0.05 M H_2SO_4 solution, the electrode covered with this Cu adlayer was rinsed to remove Cu^{2+} from the solution film, and placed into a

deoxygenated 1.0 mM K_2PtCl_4 in 50 mM H_2SO_4 solution. After a 1–2 min immersion to allow the complete replacement of Cu by Pt, the electrode was rinsed again. All these operations were carried out in a multi-compartment cell in a N_2 atmosphere that prevents the oxidation of Cu adatoms in contact with O_2. Pd nanoparticles were first deposited on glassy carbon RRDE with a Pt ring, and then a Pt monolayer was deposited using the same procedure described above for single crystals. Finally, the electrode was covered with a small amount of a Nafion solution and dried in air before the RRDE measurements.[10] Solutions were prepared from Optima* sulfuric acid obtained from Fisher and MilliQ UV-plus water (Millipore). An Ag/AgCl/KCl(3M) leak-free electrode was used as a reference. All potentials are quoted with respect to a reversible hydrogen electrode (RHE).

In situ scanning tunneling microscopy (STM) study was performed using a Molecular Imaging Pico STM with a 300S scanner and a 300S Pico Bipotentiostat. The tunneling tips were made of a polycrystalline Pt–20 % Ir wire and coated with Apiezon wax. The cell was made of Teflon, and Pt wires served as the reference and counter electrodes.

The electrochemical cell for XAS was designed for data acquisition in both transmission and fluorescence modes.[25] A Pt/Pd/C catalyst electrode, a proton exchange membrane (Nafion 117, DuPont Chemical Co., DE), and a carbon counter electrode (Grafoil, Union Carbide Corp.) were sandwiched together and held in PTFE gaskets. An electrolyte 1 M $HClO_4$ was added to the cell to increase the wetting of the sample. It did not affect the measurements because of its low X-ray absorption and anion adsorption characteristics. The total amount of Pt in the Pt/Pd/C electrode was *ca*. 0.7 mg/cm^2, small enough to avoid self-adsorption in fluorescence-type measurements. XAS measurements were carried out at the National Synchrotron Light Source (NSLS), Brookhaven National Laboratory (BNL) using Beam Line X11A and X-9B. The measurements were carried out in the fluorescence mode at the Pt L_3 and L_2 edges at different potentials at room temperature.

RESULTS AND DISCUSSION

As an example of the results obtained for a Pt monolayer deposition on single crystal electrodes we show the data for an Rh(111) surface. Figure 1a shows the typical voltammetry curve with two peaks for the upd of Cu on a Rh(111) surface. The charge associated with these peaks is 540 μC/cm^2, which is close to 524 μC/cm^2, needed for depositing a pseudomorphic monolayer of Cu on an ideal Rh(111) surface. The most negative peak is very close to the bulk deposition of Cu, which imposes careful control of the Cu upd deposition to avoid deposition of more than a monolayer of Cu. This is critical since the amount of deposited Pt corresonds to the upd Cu coverage. The dashed line shows the curve for a Rh(111) surface in the absence of Cu ions in solution. Figure 1b depicts the voltammetry curves for the Pt monolayer on a Rh(111) surface (solid line) and that for a Rh(111) surface without Pt (dashed line). As expected, the deposition of the Pt monolayer partially block oxide formation on Rh(111) since Pt is oxidized at more positive potentials.

Figure 2 is the STM image of the Pt monolayer deposited using a galvanic displacement of a Cu monolayer on a Rh(111) surface obtained at 0.8 V in 0.1 M $HClO_4$ solution. The deposit consists of two-dimensional interconnected Pt islands. With the small difference between the Pt and Rh latice constants, these islands are expected to be epitaxial with the Rh(111) substrate. There are a certain number of holes between the islands, and also a few sites with Pt atoms in the second layer. Similar deposits were obtained with the other substrates used for this study.

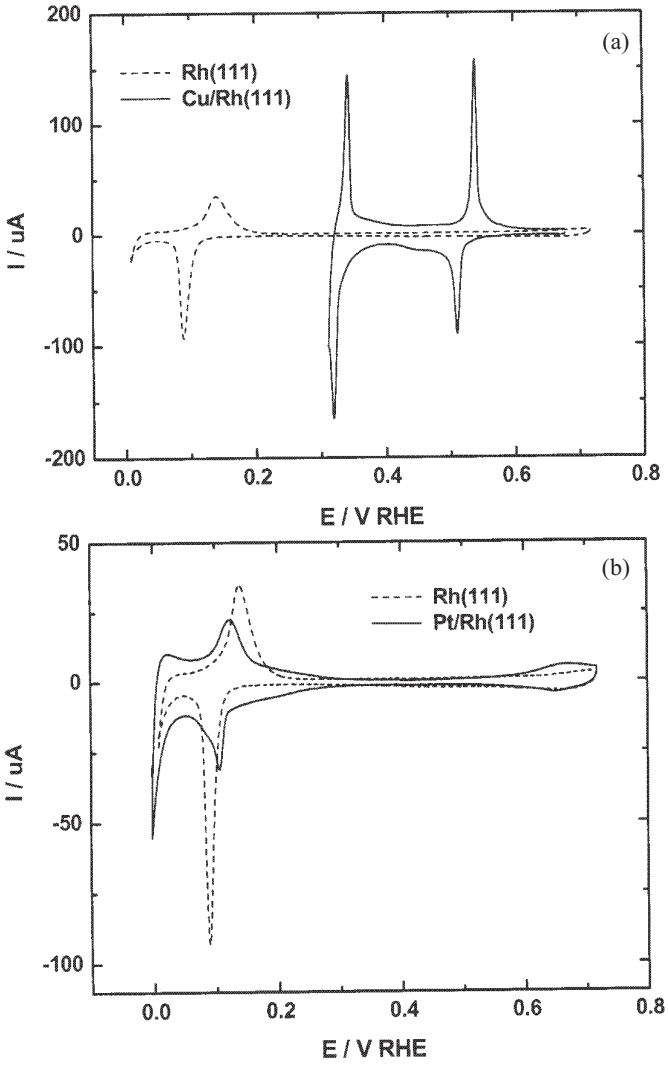

Fig. 1 (a) Voltammetry curves for the underpotential deposition of Cu on a Rh(111) surface (solid line) in 0.05 M H_2SO_4 with 0.05 M Cu^{2+}, and without Cu^{2+} (dashed line); sweep rate 20 mV/s. (b) Voltammetry curves for a Pt monolayer on a Rh(111) surface (solid line) obtained by galvanic displacement of the Cu monolayer from Fig. 1a, and for a Rh(111) surface (dashed line). The electrolyte solution is 0.05 M H_2SO_4 and the sweep rate is 20 mV/s.

Figure 3 shows the rotating disk–ring measurements for O_2 reduction on Pt monolayers on the five different single crystal surfaces and, for comparison, on a Pt (111) surface taken from the Reference 26. The most active surface is Pt_{ML}/Pd(111), and the least active is Pt_{ML}/Ru(0001). The oxidation at the ring electrode of H_2O_2 generated by ORR at the disk was measured by keeping its potential at 1.1V where the reaction is under diffusion control. Less active electrodes generated a larger amount of H_2O_2. However, O_2 reduction involves a four-electron reduction on all Pt surfaces, including the least active Pt/Ru(0001)[27] where 6.8 % H_2O_2 is generated at the peak current. Therefore, the overal reaction can be written as

$$O_2 + 4H^+ + 4e^- = 2H_2O \quad (1)$$

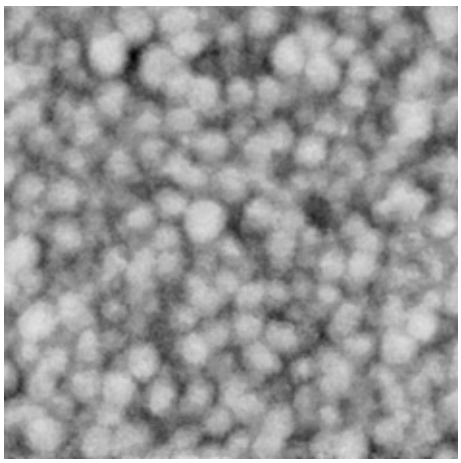

Fig. 2. An *in situ* STM image of a Pt monolayer on a Rh(111) surface obtained at 0.8 V in 0.1 M $HClO_4$ solution. Image size is 47 x 47 nm, *Z* range 3 nm.

Analysis involving the Koutecky–Levich plots and Tafel slopes indicates that the reaction is a first order one for the concentration of dissolved O_2 and that the

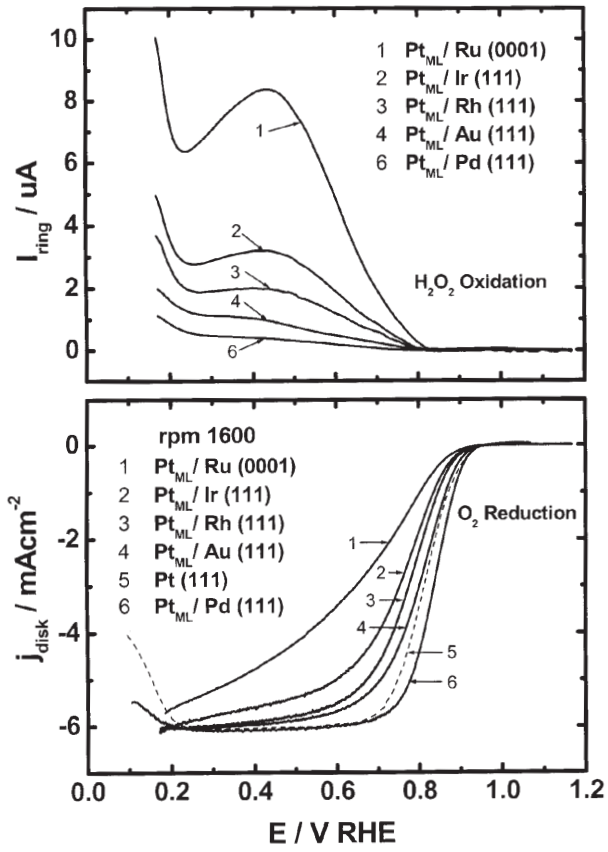

Fig. 3. Polarization curves for O_2 reduction on Pt monolayers on Ru(0001), Ir(111), Rh(111), Au(111), and Pd(111) in a 0.1 M $HClO_4$ solution on a disk electrode (lower panel). The curve for Pt(111) included for comparison is from Ref. 18. The rotation rate is 1600 rpm, sweep rate is 20 mV/s (50 mV/s for Pt(111)). The currents for H_2O_2 oxidation on a ring electrode as a function of the disk potential (upper panel); ring potential is 1.1 V, and collection efficiency is 0.20.

first charge-transfer is rate determining. Therefore, it is highly likely that the reaction mechanism is same for Pt monolayers on all five substrates investigated. Accordingly, comparison of the O_2 reaction rates on these surface is a reliable and valid procedure.

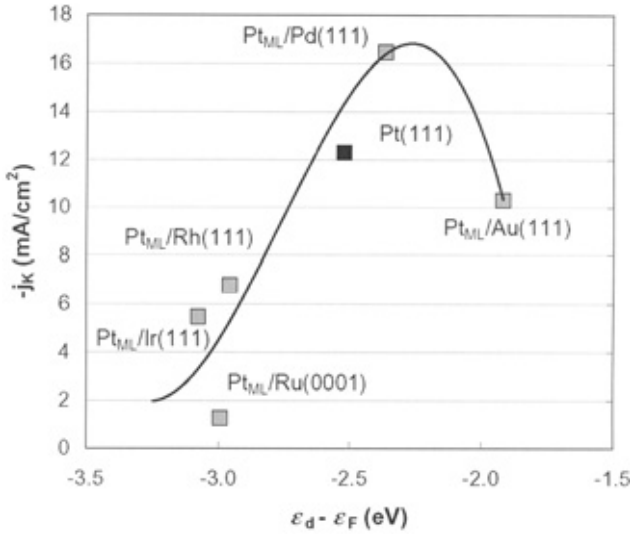

Fig. 4. Kinetic currents at 0.8 V for O_2 reduction on the Pt monolayers supported on the indicated single crystal surfaces in a 0.1 M $HClO_4$ solution and calculated binding energies (B.E.s) of atomic oxygen as functions of calculated d-band center (ε_d) of the respective clean Pt monolayers. The data for (ε_d) obtained from Ref. 28.

Plotting the kinetic currents obtained from Koutecky–Levich plots (not shown) for O_2 reduction on the Pt monolayers on various substrates at 0.8 V as a function of the calculated d-band centers for Pt monolayers, ε_d (Fig. 4), produces a volcano-like curve, with Pt_{ML}//Pd(111) possessing the maximum activity.[28] This increase in O_2 reduction kinetics on Pt_{ML}/Pd(111) compared with that on Pt(111) is surprising since Pt(111) and Pt(110) are the most active electrocatalysts for ORR known so far in $HClO_4$ solutions. As Xu *et al.* demonstrated,[21] a more reactive surface, such as one charcterized by a higher-lying ε_d, tends to bind adsorbates more strongly, thereby enhancing the kinetics of O_2 dissociation reactions. On the other hand, a surface with a lower-lying ε_d tends to bind adsorbates more weakly and facilitates the formation of bonds between them. Too strong an adsorption of intermediates for Pt/Au(111), the surface with the highest ε_d (the most stretched Pt lattice), causes a decrease in activity. The observed increase in the catalytic activity of the Pt monolayer surfaces on Pd substrates compared with those on Pt may also partly reflect the decreased formation of PtOH on Pd-supported Pt monolayers (*vide infra*).

Activity of oxygen reduction at a Pt monolayer on C-supported Pd nanoparticles

Figure 5 shows polarization curves of O_2 reduction on Pd and Pt nanoparticles (10 nmol each) and on a Pt monolayer on Pd nanoparticles (10 nmol and 20 nmol Pd) at a rotation rate of 1600 rpm.[10] In these measurements, the ring-elcectrode currents were negligible. TEM measurement showed an average diameter of 9 nm for the Pd nanoparticles used for the Pt/Pd/C electrocatalyst. Comparing the activity of the Pt/C electrocatalyst with an average particle size of 3.1 nm with that of the 9 nm Pt/Pd/C electrocatalyst does not adequately reflect the difference in their activities because of their different surface areas. However, this does not affect our main conclusion, as follows. The activity of the Pt monolayer on Pd nanoparticles

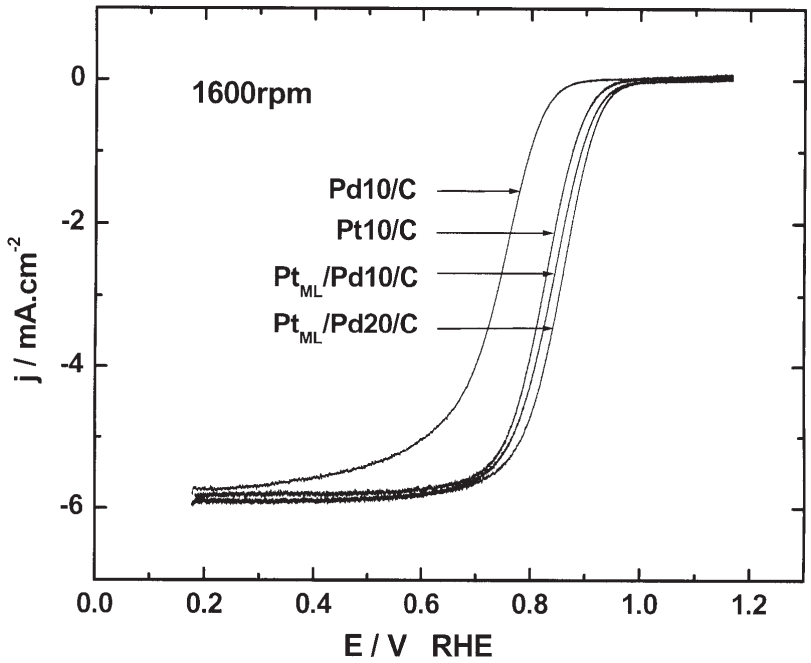

Fig. 5. Comparison of polarization curves for O_2 reduction on Pd(10 nmol) and Pt(10 nmol) nanoparticles, and a Pt monolayer on Pd nanoparticles (10 and 20 nmol Pd). The electrode geometric area is 0.164 cm^2.

(10 nmol) is much higher than that of Pd nanoparticles (10 nmol) as indicated by a shift of the half-wave potential by 120 mV to positive values. More importantly, the activity of this surface is somewhat higher (25 mV in half-wave potential) than that of Pt nanoparticles (10 nmol). For the Pd loading of 10 nmol or 6.4 $\mu g_{Pd}/cm^2$, the amount of Pt in the monolayer on this surface is 1.5 nmol/cm^2 or 1.7 $\mu g_{Pt}/cm^2$, based on Benfield's calculation using an icosahedral particle model.[29] The half-wave potential for this electrode is 0.838 V. Importantly, we note that the activity of this surface is higher than that of 10 nmol (12 $\mu g_{Pt}/cm^2$) of Pt nanoparticles, despite the fact that average diameters of the Pd nanoprticles and the Pt nanoparticles are 9 nm and

3 nm, respectively, and the former have a smaller real surface area. The electrode consisting of a Pt monolayer on 20 nmol Pd had the highest activity, mainly due to the increased Pt surface area. The higher activity of the Pt monolayer electrocatalysts compared with those of Pt and Pd indicate a synergetic effect of Pt and Pd, which is particularly interesting since the activity of the Pt/Pd surface surpasses that of Pt nanoparticles with a seven times larger loading.

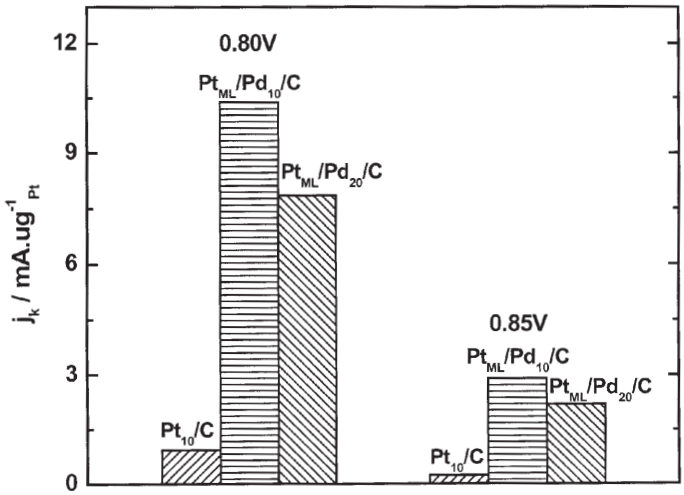

Fig. 6. Pt mass-specific activities of Pt (10 nmol) nanoparticles, and a Pt monolayer (1.3 and 2.4 nmol) on Pd nanoparticles (10 and 20 nmol Pd) expressed as a current at 0.8 and 0.85 V.

In addition to the polarization curves, a useful way of comparing the activities of electrocatalysts is by their mass-specific activities. Figure 6 shows the Pt mass-specific activity of the three electrodes containing Pt expressed as the current at 0.85 and 0.80 V divided by the Pt mass.[10] The Pt mass-specific activity of the Pt/Pd/C electrode is 5–8 times higher than that of the Pt/C electrocatalyst. The noble metal (Pt + Pd) mass-specific activity, defined as the current at given potential divided by total noble metal mass (Pt + Pd) is twice as high as that of Pt/C.[10] This finding underlines the importance of the monolayer-level electrocatalysts that can greatly lower the amount of Pt in the fuel cell's electrode.

Decreased oxidation of Pt on Pd

As described in the introduction, one of the problems for O_2 electrocatalysis is the large potential loss in the initial part of the polarization curve, which is a source of major inefficiency. The initial potential loss was partly attributed to inhibitory effect of OH adsorption on Pt at very positive potentials.[3,5] The role of adsorbed OH (PtOH) is controversial. It was considered to be the reaction intermediate,[10] but several workers proposed that PtOH is not derived from the reduciton of O_2 but rather from the reaction of H_2O with Pt, thereby inhibiting the ORR.[31–33] Recently, we demonstrated that PtOH had a negative electronic effect on O_2 reduction kinetics, in addition to site blocking.[34] To quantitatively evalute these effects of the

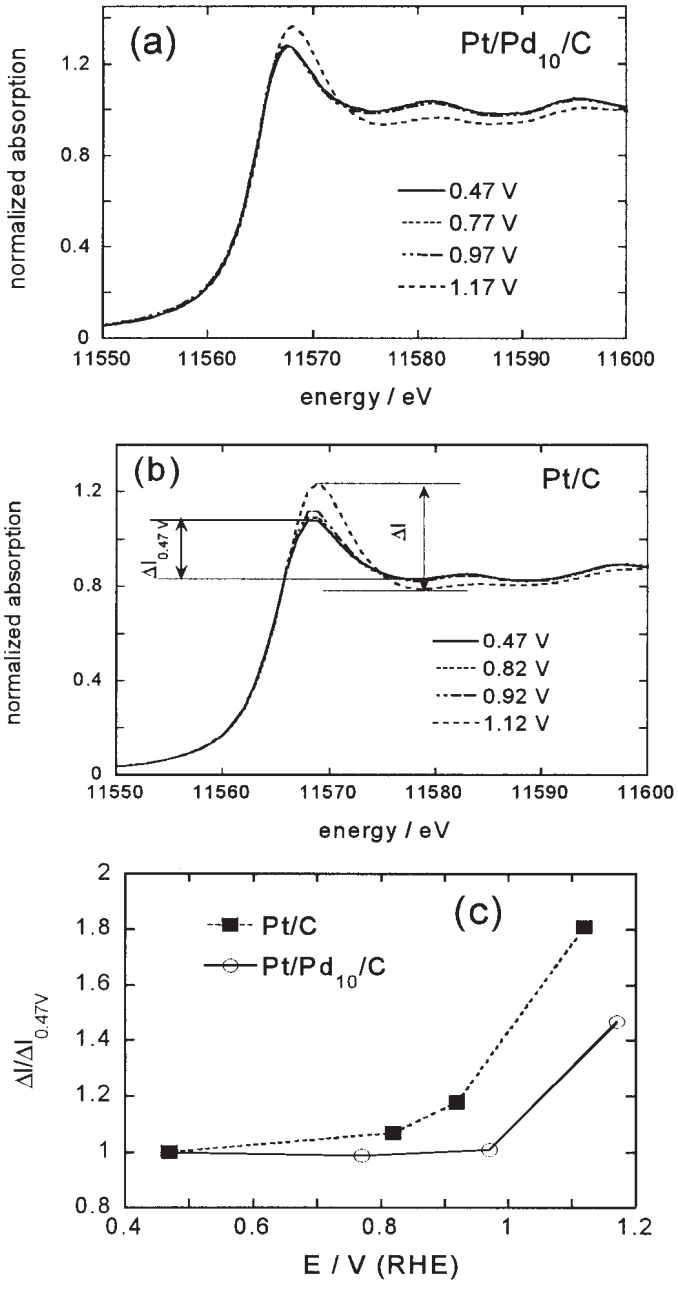

Fig. 7. XANES spectra obtained with the $Pt/Pd_{10}/C$ (a) and Pt/C (b) electrocatalysts at four different potentials in 1 M $HClO_4$. (c) A comparison of the change of the absorption peak as a function of potential for $Pt/Pd_{10}/C$ and Pt/C expressed as a ratio of peak value at given potential and the peak value at 0.47 V.

PtOH species, the following equation was used,[34]

$$j_k(E) = -j^*_0 (1 - \gamma_{OH}\theta_{OH}(E))^m \exp(2.303(E - E^\circ - \varepsilon_{OH}\theta_{OH}(E))/b^*) \quad (2)$$

where j_0^* and b^* are, respectively, the intrinsic exchange current and Tafel slope for an adsorbate-free Pt surface. The $(1 - \gamma\theta)^m$–term accounts for the geometric site-blocking effect, while the electronic effect is desribed by a coverage-dependent potential shift through the exponential term, "$\varepsilon\theta$", and m is the number of Pt sites involved in the rate-determining step. Equation (2) shows that a decrease in the coverage of PtOH can enhance the kinetics of O_2 reduction.

As discussed above, the observed increase in the catalytic activity of the Pt monolayer surfaces on Pd nanoparticles compared with the Pt nanoparticle electrodes appears to be caused partly by decreased formation of PtOH. This is in accord with the results of the DFT calculations[28] which show a slightly smaller reactivity. Clear evidence of delayed oxidation of a Pt monolayer on Pd nanoparticles compared with the oxidation of Pt nanoparticles was obtained from *in-situ* XANES measurements as a function of potential. Figure 7a shows the Pt L_3 edge spectra obtained with the $Pt/Pd_{10}/C$ electrocatalysts at four differenent potentials. Only at the highest potentials there is an increase in the intensity of white line (edge peak) as a consequence of the formation of PtOH depleting Pt's-band.[35] The increase in the intensity of the white line for the Pt/C electrocatalyst commences at considerably less positive potentials (Figure 7b). This demonstrates that the oxidation of a Pt monolayer on Pd substrate requires higher potentials than do Pt nanoparticles on a carbon substrate. Figure 7c compares the change of the absorption peak as a function of potential for $Pt/Pd_{10}/C$ and Pt/C expressed as a ratio of peak value of given potential and the peak value at 0.47 V. As seen, there is a negligible change in the electronic properties of a Pt monolayer on Pd in comparison with Pt/C. No effect of the potential change is observed below 1 V. This suggests that PdOH plays a role in suppressing a PtOH formation.[10] Pd is more easily oxidized than Pt and the coverage of PdOH already is high before PtOH formation commences. Repulsion between PtOH and PdOH delays the oxidation on Pt. This view is confirmed by the behavior of mixed monolayer on Pd(111).[36] We note that voltammetry also recorded the decrased formation of PtOH on the Pt/Pd/C electrocatalysts with increasing potentials.[10]

Long-term stability of a Pt monolayer on Pd nanoparticles

The long-term stability tests were carried out using the fuel cell with electrodes of 50 cm^2 in area. The cathode was Pt/Pd/C catalyst containing 77 $\mu g/cm^2$ of Pt (0.21 g/kW of Pt) and 385 $\mu g/cm^2$ of Pd. Figure 8 illustrates the trace of the cell voltage at a constant current of 0.6 A/cm^2 against time at 80 °C. Up to 1000 h, the cell voltage dropped about 120 mV, and then showed a much lower rate of decrease with time. The total loss in voltge was approximately 130 mV at 2300 h, the end of the test. Cyclic voltammetric measurements occasionally were made during the test to investigate changes in active

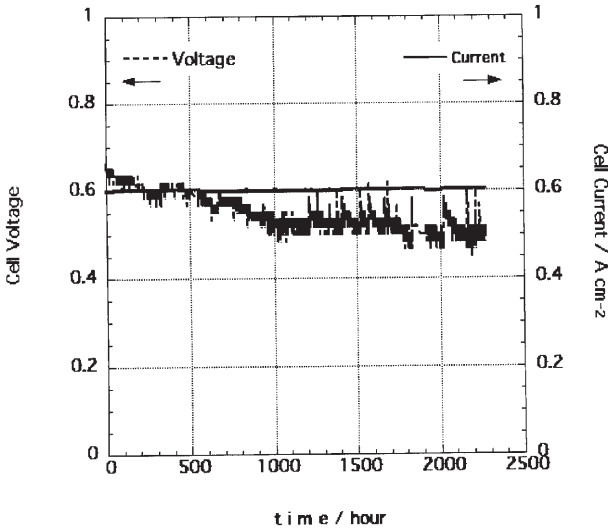

Fig. 8. Long-term stability test of the Pt/Pd electrocatalyst in an operating fuel cell at 80 °C. The fuel-cell voltage at a constant current of 0.6 A/cm^2 is plotted as a function of time with a cathode containing 385 μg/cm^2 of Ru, and 77 μg/cm^2 of Pt (or 0.21 g/kW of Pt). A commercial Pt/C electrocatalyst (180 μg/cm^2 of Pt) was used for an anode.

surface area of Pt in the cathode from charges determined by hydrogen adsorption/desorption peaks. This indicated losses of the active Pt surface area, by approximately 26 % at 1200 h and 29 % at 2000 h compared with the initial surface area before testing. These losses in Pt could reflect the dissolution of Pt at the operating potential, or the embedding of Pt atoms into the Pd substrate. The latter is predicted by the anti-segregation of Pt from Pd according to DFT calculations.[19] We note that a part of the observed drop in voltage also may be due to losses at the anode (a commercial Pt/C elecrocatalyst) since the measurements did not separate the losses at the anode and cathode in these fuel cells. The results are promising but further investigation is necessary to improve the long-time durability of the electrocatalyst.[36]

CONCLUSIONS

The kinetics of O_2 reduction was studied on Pt monolayers deposited on the surface of Au(111), Ir(111), Pd(111), Rh(111) and Ru(0001) single crystals, and Pd nanoparticles. There was a small enhancement of the activity of this Pt monolayer on Pd substrates compared with that of Pt electrocatalysts. The ORR electrocatalytic activity of Pt monolayers supported on the single crystal surfaces showed a volcano-type dependence on the d-band center of the Pt monolayer structures.[28] The heightened activity is partly attributed to a decreased OH adsorption shown by *in situ* XANES experiments.

Our findings demonstrate that the approach of placing sub-monolayer-monolayer Pt on a suitable nanoparticle substrate is an attractive way of designing ultra-low Pt loading electrocatalysts with improved ORR performance.

Acknowledgemements: This work was supported by US. Department of Energy, Divisions of Chemical and Material Sciences, under the Contract No. DE-AC02-98CH10886.

ИЗВОД

ЕЛЕКТРОКАТАЛИЗАТОРИ ЗА РЕДУКЦИЈУ КИСЕОНИКА СА ПЛАТИНСКИМ МОНОСЛОЈЕМ. УТИЦАЈ СУБСТРАТА И ПОСТОЈАНОСТ У ВРЕМЕНУ

J. ZHANG,[1] М. Б. ВУКМИРОВИЋ,[1] K. SASAKI,[1] F. URIBE[2] и Р. Р. АДЖИЋ[1]

[1]Department of Materials Science, Brookhaven National Laboratory, Upton, NY 11973, USA и [2]Los Alamos National Laboratory, Los Alamost, NM 87545, USA

Описан је нов концепт добијања електрокатализатора који чине само монослој Pt на носачу, илустрован резултатима добијеним електрохемијским техникама, апсорпционом спектроскопијом X-зрака и скенирајућом тунелском микроскопијом. Електрокатализатори су синтетизовани новим методом депозиције Pt монослоја који се састоји од галванске замене Pt монослојем Cu депонованог на подпотенцијалима на Au(111), Ir(111), Pd(111) и Ru(0001) монокристалима и Pd наночестицама. Показано је значајно увећање кинетике редукције кисеоника на Pt монослоју на Pd(111) и Pd наночестицама у поређењу са Pt(111) и Pt наночестицама. Повећање каталитичке активности је делимично проузроковано умањеним стварањем PtOH, што је показано апсорпционом спектроскопијом X-зрака. Резултати показују да је депозиција Pt монослоја на одговарајуће металне наночестице примамљив начин синтезе бољих катализатора за редукцију кисеоника са минималном количином Pt.

(Примљено 16. децембра 2004)

REFERENCES

1. W. Vielstich, A. Lamm, and H. A. Gestiger, Eds. *Handbook of Fuel Cells: Fundmaentals, Technology and Application*, Wiley, West Sussex, 2003
2. M. R. Tarasevich, A. Sadkowski, E. Yeager, in *Comprehensive Treatise of Electrochemistry,* vol. 7, B. E. Conway, J. O. Bockris, E. Yeager, S. U. M. Khan, R. E. White, Eds., Plenum Press, New York, 1983, Vol. 7, p. 301
3. R. R. Adžić, in *Electrocatalysis*, J. Lipkowski and P. N. Ross, Eds. VCH Publishers, New York, 1998, Vol. 5, p. 197
4. S. Gottesfeld, T. A. Zawodzinski, in *Advances in Electrochemical Science and Engineering*, R. C. Alkire and D. M. Kolb, Eds., Wiley-VCH, Weinham, 1997, Vol. 5, p. 195
5. A. Anderson, *Electrochim. Acta* **47** (2002) 3759
6. J. X. Wang, S. R. Branković, R. R. Adžić, *Electrochem. Solid-State Lett.* **4** (2001) A217
7. S. R. Branković, J. X. Wang, Y. Zhu, R. Sabatini, J. McBreen, R. R. Adžić, *J. Electroanal. Chem.* **524** (2002) 231
8. J. X. Wang, S. R. Branković, Y. Zhu, J. C. Hanson, R. R. Adžić, *J. Electrochem. Soc.* **150** (2003) A1108
9. K. Sasaki, Y. Mo, J. X. Wang, M. Balasubrmanian, F. Uribe, J. McBreen, R. R. Adžić, *Electrochim. Acta* **48** (2003) 3841
10. J. Zhang, Y. Mo, M. B. Vukmirović, R. Klie, K. Sasaki, R. R. Adžić, *J. Phys. Chem. B* **108** (2004) 10955
11. S. R. Branković, J. X. Wang, R. R. Adžić, *J. Serb. Chem. Soc.* **66** (2001) 887
12. K. Sasaki, J. X. Wang, M. Balasubramanian, J. McBreen, F. Uribe, R. R. Adžić, *Electrochim. Acta* **49** (2004) 3873
13. S. R. Branković, J. X. Wang, R. R. Adžić, *Surf. Sci.* **474** (2001) L173
14. J. A. Rodriguez, *Surf .Sci. Rep.* **24** (1996) 225
15. M. Baldauf, D. M. Kolb, *J. Phys. Chem.* **100** (1996) 11375
16. H. Naohara, S. Ye, K. Uosaki, *Electrochim. Acta* **45** (2000) 3305

17. R. R. Adžić, in *Encyclopedia of Electrochemistry,* A. Bard and M. Stratmann, Eds., Wiley-VCH, New York, 2002, Vol. 1
18. T. J. Schmidt, V. Stamenković, M. Arenz, N. M. Marković, P. N. Ross, *Electrochim. Acta* **47** (2002) 3765
19. B. Hammer, J. K. Nørskov, *Adv. Catal.* **45** (2000) 71
20. J. Greeley, J. K. Nørskov, M. Mavrikakis, *Annu. Rev. Phys.* **53** (2002) 319
21. Y. Xu, A. V. Ruban, M. Mavrikakis, *J. Am. Chem. Soc.* **126** (2004) 4717
22. J. A. Rodriguez, D. W. Goodman, *Science* **257** (1992) 897
23. F. B. de Mongeot, M. Scherer, B. Bleich, E. Kopatzki, R. J. Behm, *Surf. Sci.* **411** (1998) 249
24. E. Christoffersen, P. Liu, A. Ruban, H. L. Skiver, J. K. Nørskov, *J. Catal.* **199** (2001) 123
25. J. McBreen, W. E. O'Grady, K. I. Pandy, R. W. Hoffmna, D. E. Sayers, *Langmuir* **3** (1987) 428
26. N. M. Marković, H. A. Gasteiger, B. N. Grgur, P. N. Ross, *J. Electroanal. Chem.* **467** (1999) 157
27. H. Inoue, S. R. Branković, J. X. Wang, R. R. Adžić, *Electrochim. Acta* **47** (2002) 3777
28. J. Zhang, M. B. Vukmirović, X. Ye, M. Mavrikakis, R. R. Adžić, *Angew. Chem. Int. Ed.,* **44** (2005) 2
29. R. E. Benfield, *J. Chem. Soc., Faraday Trans.* **88** (1992) 1107
30. A. Damjanović, M. A. Genshaw, J.O'M. Bockris, *J. Phys. Chem.* **45** (1964) 4057
31. M. R. Tarasevich, *Elektrokhimiya* **9** (1973) 578
32. R. R. Adžić, in *Structural Effects in Electrocatalysis and Oxygen Electrochemistry*, Proc., Scherson, D. D.; Tryk, D.; Xing, X. Eds. Pennington: the Electrochem. Soc. Inc., 1992, Vol. 92–11, p. 419
33. F. A. Uribe, M. S. Wilson, T. E. Springer, S. Gottesfeld, in *Structural Effects in Electrocatalysis and Oxygen Eletrochemistry*, Proc. Scherson, D. D.; Tryk, D.; Xing, X. Eds.; Pennington: The Electrochem. Soc. Inc., 1992, Vol. 92–11, p. 494
34. J. X. Wang, N. M. Marković, R. R. Adžić, *J. Phys. Chem.* **108** (2004) 4127
35. S. Mukerjee, S. Srinivasan, M. Soriaga, J. McBreen, *J. Electrochem. Soc.* **142** (1995) 1409
36. J. Zhang, M. B. Vukmirović, A. U. Nilekar, M. Mavrikakis, R. R. Adžić in preparation.